International Journal of Medical, Medicine and Health Sciences
ISSN: 2517-9969
Vol:12, No:5, 2018

Replicating Brain's Resting State Functional Connectivity Network Using a Multi-Factor Hub-Based Model

B. L. Ho, L. Shi, D. F. Wang, V. C. T. Mok

Abstract**—**The brain's functional connectivity while temporally non-stationary does express consistency at a macro spatial level. The study of stable resting state connectivity patterns hence provides opportunities for identification of diseases if such stability is severely perturbed. A mathematical model replicating the brain's spatial connections will be useful for understanding brain's representative geometry and complements the empirical model where it falls short. Empirical computations tend to involve large matrices and become infeasible with fine parcellation. However, the proposed analytical model has no such computational problems. To improve replicability, 92 subject data are obtained from two open sources. The proposed methodology, inspired by financial theory, uses multivariate regression to find relationships of every cortical region of interest (ROI) with some pre-identified hubs. These hubs acted as representatives for the entire cortical surface. A variance-covariance framework of all ROIs is then built based on these relationships to link up all the ROIs. The result is a high level of match between model and empirical correlations in the range of 0.59 to 0.66 after adjusting for sample size; an increase of almost forty percent. More significantly, the model framework provides an intuitive way to delineate between systemic drivers and idiosyncratic noise while reducing dimensions by more than 30 folds, hence, providing a way to conduct attribution analysis. Due to its analytical nature and simple structure, the model is useful as a standalone toolkit for network dependency analysis or as a module for other mathematical models.

Keywords**—**Functional magnetic resonance imaging, multivariate regression, network hubs, resting state functional connectivity.

I. Introduction

THE resting human brain is highly significant for understanding how the brain works [1] as reflected by the energy-mass consumption distribution; the resting brain accounts for 20% of the human energy consumption [1] despite its disproportionately small mass. Although calculation of brain spatial correlation is simple, there are various challenges. First, large amount of calculations limits the granularity of the parcellation scheme. Second, the spontaneous resting state signals used for calculations are not temporally stationary, making topology mapping difficult [2].

In [3], various mathematical approaches have been tested and compared. Methods by Galán [4] and Honey et al. [5], achieve mean correlations of 0.33 and 0.36, respectively. Both methods use discrete time-simulation which tend to be slow and require many simulations before stabilizing. An analytical network diffusion model by Abdelnour et al. [3] achieved a correlation of 0.41 for eight subjects when tested within the same context. Although relatively superior in performance, the method assumes prior knowledge of a hyperparameter, βt, which is retrospectively optimized based on the value that produces the most favorable matching outcome. Since only eight subjects were used for optimization, likelihood of under-estimation of inter-subject variability is high.

B. L. Ho is with the Department of Medicine and Therapeutics, The Chinese University of Hong Kong, Shatin, Hong Kong, China (corresponding author, phone: +852 92402283; e-mail: 1155102310@ link.cuhk.edu.hk).

L. Shi and D. F. Wang are with the Department of Imaging and Interventional Radiology, The Chinese University of Hong Kong, Shatin, Hong Kong, China (e-mail: shilin@ cuhk.edu.hk).

V. C. T. Mok is with the Department of Medicine and Therapeutics, The Chinese University of Hong Kong, Shatin, Hong Kong, China.

II. Theory

The model proposed here is inspired by the financial asset return theory in the world of stocks [6]. In finance, it is not uncommon to model an individual stock's return based on several systematic factors. Covariance of one stock with another is often prescribed by a set of key drivers such as global stock index, regional stock index and other systematic drivers such as oil price, exchange rates, etc. One will find that some stocks' performances are particularly well-explained by systematic drivers while others such as small stocks are largely driven by its own idiosyncrasies. Similarly, one can hypothesize that the different regions of interests (ROI) of brain are dependent on some key hubs. Regardless of its functionality, it is unlikely any ROI to be totally independent of other hubs or limited in dependency to just 1 hub. Where there is a general dependency of each ROI to 2 or more hubs, the conditions may be favorable for the usage of this model. The model uses a simple multivariate regression of every ROI with a set of chosen network representatives [6]. The starting hypothesis is that every ROI is somehow driven to different extent by a few core representatives. If a relationship of every ROI with these representatives can be established, it may also be possible to establish indirect relationship of ROIs amongst themselves. For illustration purposes, Fig. 1 provides a schema for this framework.

Mathematical derivation in later section demonstrates how one can leverage on a fixed choice of factors to account for covariation between stocks or in this case, different parts of the grey matter.

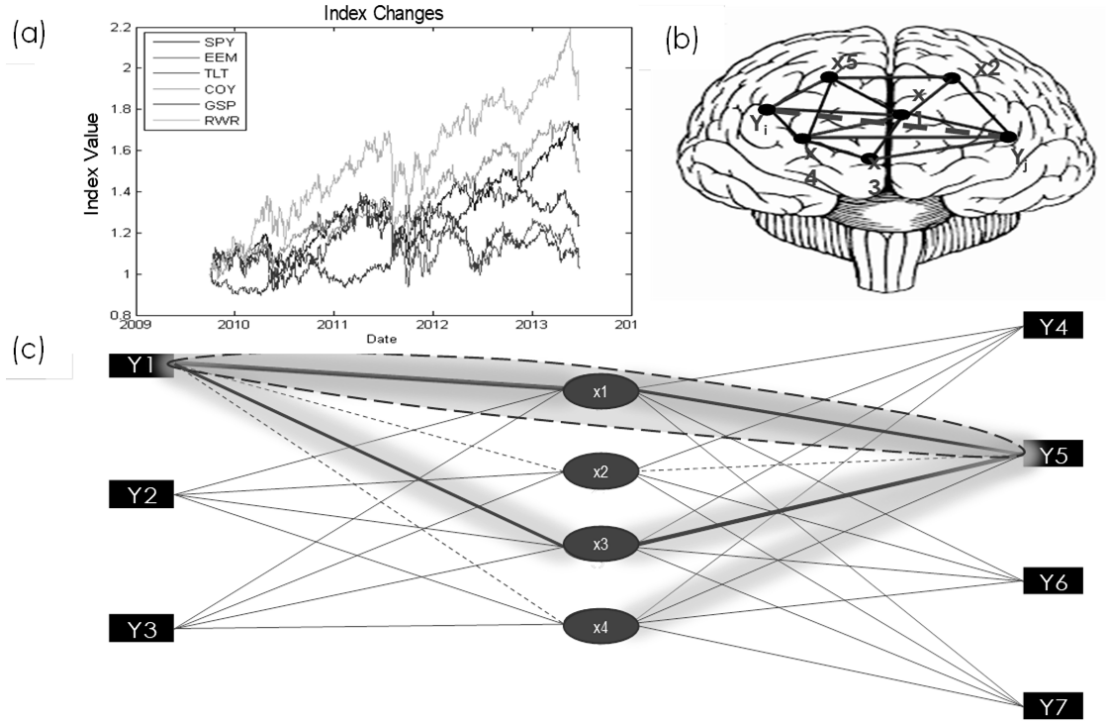

Fig. 1 Schematics of indirect connectivity through key hubs. A) Example of how different stock indices are correlated to different extent, allowing a target index to be expressed as a function of the other indices. B) A schema of how key hubs of the brain (represented by Xs) could be used to link up the different ROIs (Ys). C) A schema further showing how two ROIs (Y1 & Y5) are indirectly connected through their linkages to hubs, X1 to X4. Solid lines here represent significant connectivity whereas dotted lines represent weak connectivity with insignificant strength of connection

A. Notations

Let $Y_{1,t}$, $Y_{2,t}$, …,$Y_{N,t}$ be the levels of spontaneous activity at time, t for N ROIs after standard image preprocessing and additional signal preprocessing associated with rs-fMRI analysis. Let $X_{1,t}$, $X_{2,t}$, $X_{3,t}$, …,$X_{K,t}$ be a choice of K factors such that $X \in Y_i$, where i = 1 to N. To account for different subjects, the notations are adjusted accordingly:

Xs and Ys become $X_{k,t}^j$ and $Y_{i,t}^j$, where j refers to the index for a subject $j \in [1, J]$ and J is the number of subjects. $t \in [1, T]$, where t refers to time index when the spontaneous activity is recorded, and T refers to the index where the last spontaneous activity is recorded. A full multivariate setup is as shown below where $\varepsilon_{i,t}^j$ refers to zero-mean Gaussian and where variance is not necessarily unit. i, j, k follows the set notations described earlier.

$$Y_{i,t}^j = \beta_{i,0} + \beta_{i,1}X_{1,t}^j + \beta_{i,2}X_{2,t}^j + \ldots + \beta_{i,k}X_{k,t}^j + \varepsilon_{i,t}^j \quad (1)$$

Alternatively, in simple matrix form:

$$\begin{bmatrix} Y_{i,.}^1 \\ Y_{i,.}^2 \\ Y_{i,.}^3 \\ \vdots \\ Y_{i,.}^J \end{bmatrix} = \begin{bmatrix} X_{1,.}^1 X_{2,.}^1 \ldots X_{K,.}^1 \\ X_{1,.}^2 X_{2,.}^2 \ldots X_{1K.}^2 \\ X_{1,.}^3 X_{2,.}^3 \ldots X_{K,.}^3 \\ \vdots \\ X_{1,.}^J X_{2,.}^J \ldots X_{K,.}^J \end{bmatrix} \begin{bmatrix} \beta_{I,1} \\ \beta_{I,2} \\ \beta_{I,3} \\ \ldots \\ \beta_{I,K} \end{bmatrix} + \begin{bmatrix} \varepsilon_{I,.}^1 \\ \varepsilon_{I,.}^2 \\ \varepsilon_{I,.}^3 \\ \vdots \\ \varepsilon_{I,.}^J \end{bmatrix} \quad (2)$$

Example: $Y_{i,.}^1$ refers to a time series for subject 1, ROI i. Y is a JT x 1 vector, X is a JT x K matrix, B is a Kx1 vector, ε is a JT x 1 vector. Perform a regression for every ROI i, a set of β for each ROI will be produced. Stack them horizontally and re-arrange some of the results from regression:

$$A = cov(X) = \begin{bmatrix} \sigma_1^2 & \rho_{21}\sigma_2\sigma_1 \ldots \rho_{K1}\sigma_K\sigma_1 \\ \rho_{12}\sigma_1\sigma_2 & \sigma_2^2 \quad \ldots \rho_{K2}\sigma_K\sigma_2 \\ \rho_{13}\sigma_1\sigma_3 & \rho_{23}\sigma_2\sigma_3 \ldots \rho_{K3}\sigma_K\sigma_3 \\ \rho_{1K}\sigma_1\sigma_K & \rho_{2K}\sigma_2\sigma_K \quad \ldots \sigma_K^2 \end{bmatrix} \quad (3)$$

$$B = \begin{bmatrix} \beta_{1,1} \beta_{1,2} \ldots \beta_{1,K} \\ \beta_{2,1} \beta_{2,2} \ldots \beta_{2,K} \\ \beta_{3,1} \beta_{3,1} \ldots \beta_{3,K} \\ \beta_{N,1}\beta_{N,1} \ldots \beta_{N,K} \end{bmatrix} \quad (4)$$

$$D = \begin{bmatrix} var(\varepsilon_1) & 0 & \ldots 0 \\ 0 & var(\varepsilon_2) & \ldots 0 \\ 0 & 0 & \ldots 0 \\ 0 & 0 & \ldots 0 \\ 0 & 0 & \ldots var(\varepsilon_N) \end{bmatrix} \quad (5)$$

The subscripts of β and subscripts and superscripts of ε have been simplified without loss of generic meaning to reflect the fact that only information at the level of ROI and key factors are relevant.

B. Derivation of Linkage

A key benefit of the model is its reduction in dimensions, and the derivation of linkage framework which makes this possible is as follows:

$$Y_i = \beta_{i,1}X_1 + \beta_{i,2}X_2 + \beta_{i,3}X_3 + \ldots + \beta_{i,k}X_k + \varepsilon_i \quad (6)$$

$$Y_j = \beta_{j,1}X_1 + \beta_{j,2}X_2 + \beta_{j,3}X_3 + \ldots + \beta_{j,k}X_k + \varepsilon_j \quad (7)$$

$$E(Y_iY_j) = \mathrm{E}(\beta_{i,1}\beta_{j,1}X_1^2 + \beta_{i,2}\beta_{j,2}X_2^2 + \ldots + \beta_{i,k}\beta_{j,k}X_k^2 + \sum_{p\neq q}\beta_{i,p}\beta_{j,q}X_pX_q + \beta_{i,1}X_1\varepsilon_j + \beta_{i,2}X_2\varepsilon_j + \ldots + \beta_{i,k}X_k\varepsilon_j + \beta_{j,1}X_1\varepsilon_i + \beta_{j,2}X_2\varepsilon_i + \beta_{j,3}X_3\varepsilon_i + \ldots + X_k\varepsilon_i + \varepsilon_i\varepsilon_j)$$
$$= \beta_{i,1}\beta_{j,1}\sigma_1^2 + \beta_{i,2}\beta_{j,2}\sigma_2^2 + \ldots + \beta_{i,k}\beta_{j,k}\sigma_k^2 + \sum_{p\neq q}\beta_{i,p}\beta_{j,q}E(X_pX_q) + E(\varepsilon_i\varepsilon_j) \quad (8)$$

Assuming that Y_i, Y_j, X_p, X_q are zero-centered Gaussians for simplicity of derivations without loss of generality on the results. Also, notice that expectations of cross terms between ε and X are removed as they are assumed to be independent to each other.

If i≠j,

$$E(Y_iY_j) = \beta_{i,1}\beta_{j,1}\sigma_1^2 + \beta_{i,2}\beta_{j,2}\sigma_2^2 + \ldots + \beta_{i,k}\beta_{j,k}\sigma_k^2 + \sum_{p\neq q}\beta_{i,p}\beta_{j,q}cov(X_pX_q) \quad (9)$$

If i=j,

$$E(Y_iY_j) = \beta_{i,1}^2\sigma_1^2 + \beta_{i,2}^2\sigma_2^2 + \ldots + \beta_{i,K}^2\sigma_k^2 + \sum_{p\neq q}\beta_{i,p}\beta_{j,q}cov(X_pX_q) + Var(\varepsilon_i) \quad (10)$$

As one can see, this equation comprises of cross and coherent terms. Cross terms refer to terms where variables are different and coherent terms refer to those where variables are the same. Cross terms produce covariance of the type: $\beta_{i,p}\beta_{j,q}\rho_{p,q}\sigma_p\sigma_q$, where $p \neq q$, p, q ∈ $[1, k]$. Coherent terms produce variances of the type: $\beta_{i,p}\beta_{j,p}\sigma_p^2$, where $p \in [1, k]$. In fact, (9) & (10) can be equivalently expressed as equation 11.

$$F = cov(Y) = BAB^T + D \quad (11)$$

where A, B and D are from (3)-(5) respectively. The user can verify that (9) and (10) are the same by comparing a diagonal and non-diagonal term via the two different forms of expression. B is a factor loading NxK matrix, A is a factor covariance KxK matrix and D is a residual NxN matrix where non-diagonal values are zero. From examining the dimensions of B, all that is required when finding the correlations of F which by brute force is $(N+1)x\,N/2$, is N regressions. B is called the factor loading matrix, and D is called the idiosyncratic risk matrix.

III. Materials and Methods

A. Data Collection, Imaging Protocol and Preprocessing

The primary data (DS1) came from the Consortium for Neuropsychiatric Phenomics [7]. There are 29 males and 23 females, age ranging from 21 to 50 in the model building dataset, and the individuals were asked to think of nothing during the scans.

T1-weighted structural MR data were collected on a 3T Siemens Trio scanner, using MPRAGE-BWM protocol and scan sequence, IR. The parameters of the scan are: TR= 2.53 s, TE =0.0031 s, matrix size = 256 x 256, slice thickness = 1 mm, number of slices= 176, FOV=256 mm x 256 mm, total scan time=363 s, flip angle=7 deg. The fMRI scans were collected using the same scanner with echo planar sequence using the following the parameters: TR=2 s, TE=0.03 s, matrix size=64 x 64, slice thickness=4 mm, number of slices=34, slice sequence=interleaved, total scan time=312 s, flip angle=90 deg, number of time points=152 (before removal of first 10 points). Subjects are asked to think of nothing during the scans.

The secondary dataset (DS2) was collected from '1000 Functional Connectomes' database. The data chosen were contributed by Wang et al. [8]. To create a test set that allows results stabilization, 40 out of 198 subjects are chosen, with 17 males and 23 females, age ranging from 18 to 26.

The parameters for the anatomical MRI scan are: TR=2.53 s, TE =0.00339 s, matrix size=181 x 175, slice thickness=1.33 mm, number of slices=128, FOV=181 mm x 175 mm, slice order=interleaved and subjects are asked to think of nothing. The parameters of the fMRI scan are: TR=2 s, TE =0.03 s, matrix size=64 x 64, slice thickness=3.6mm, number of slices=33, FOV=200mm x 200mm, slice order=interleaved, number of time points=225, eyes closed.

The preprocessing steps are carried out using DPABI [9], an extended toolbox of SPM [10]. Steps are executed out in the following chronological order: time slice adjustment, realignment, co-registration, unified segmentation, normalization, smoothing, linear de-trending, band pass filtering (0.01~0.1 Hz) and nuisance covariates removal (white matter and CSF). In addition to standard preprocessing steps, the following processing steps are performed. All fMRI images (after covariate regression) are resliced to a resolution of [10mmx10mmx10mm] using REST toolkit [11]. Then, segmented grey matter images are averaged and resliced to [10mmx10mmx10mm] resolution and threshold at 0.3 to form a mask. The grey matter mask will form the main basis from which all comparisons between empirical and model correlations are made.

B. Factor Selection Steps

To obtain optimal hubs or representative ROIs, factors must maximize the connectivity while minimizing overlap. A 2-step heuristic is applied to achieve this:

Step 1: Hierarchical clustering. First, the average spatial correlation matrix of the subjects is computed on the grey matter ROI space, followed by the performance of hierarchical clustering. Clusters are formed using 0.7 as cut-offs which means the ROIs inside the clusters have intra-correlations of no less than 0.3. Cut-off is preferred over cluster size when forming clusters since it permits direct control over the

distance between the ROIs (correlation used as a distance metric). The clusters acted as local networks within the brain as shown in Fig. 2.

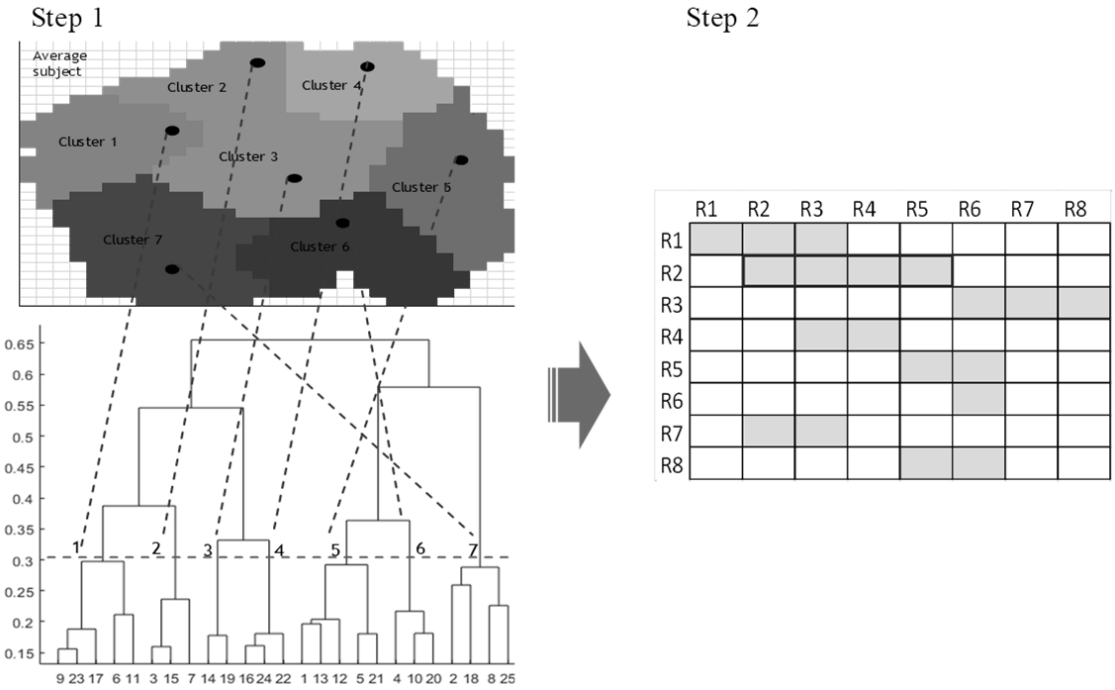

Fig. 2 Left: an illustration of using hierarchical clustering with the cut-off method to find distinct networks. Right: Illustration of correlation footprint method. If the rows represent cluster members, and cells highlighted with grey represent the extent of their influence (cell is grey if correlation is significantly different from zero). The member of the cluster with the greatest influence is the one with most number of grey cells per row

Step 2: Hubs selection. After the networks have been determined, hub representatives are chosen from them. Intuitively, it makes sense to vary the number of representatives depending on the size of the network. Over here, the optimal arrangement is for the maximum number of representatives for a cluster to be 2, while the minimum number of representatives to be 1. Small networks containing very few voxels are discarded from consideration in order to maintain parsimony and are therefore, not well represented. Representatives are chosen from their respective networks/clusters by using the correlation footprint method. This is illustrated above in Fig. 2.

IV. Results

The results using the model are superior to those previously discussed in other papers when adjusted for sample size (see Table I). As a further note, it is important to qualify that results are highly dependent on sample size up to a certain point. Right column of Tables I A and B shows results which have been stabilized while the left column is based on eight subjects to compare with the results discussed in [3].

From Fig. 3, one can also see that correlation increases with the number of factors (from 6 to 10) without decrease in adjusted R^2. Judging from the trend and given the size of the large regression sample, there is still room for further increase in performance by increasing the number of factors.

TABLE I.A
Correlation Performance for Different Number of Hubs from Sample Data Set, DS1

Set with first 8 subjects from DS1			DS1, Set with 52 subjects		
#Hubs	Correlation	Adj R-square	#Hubs	Correlation	Adj R-square
35	0.66	0.46	35	0.48	0.38
25	0.63	0.42	25	0.46	0.36
20	0.60	0.38	20	0.43	0.31
15	0.57	0.35	15	0.42	0.29
10	0.53	0.31	10	0.39	0.25
9	0.52	0.29	9	0.38	0.24
8	0.51	0.28	8	0.37	0.23
7	0.49	0.26	7	0.36	0.22
6	0.49	0.25	6	0.35	0.21

TABLE I.B
Correlation Performance for Different Number of Hubs from Sample Data Set, DS2

Set with first 8 subjects from DS2			DS2, Set with 40 subjects		
#Hubs	Correlation	Adj R-square	#Hubs	Correlation	Adj R-square
35	0.63	0.38	35	0.53	0.31
25	0.60	0.35	25	0.51	0.29
20	0.56	0.31	20	0.48	0.26
15	0.54	0.29	15	0.46	0.24
10	0.50	0.22	10	0.42	0.20
9	0.46	0.20	9	0.41	0.19
8	0.44	0.19	8	0.40	0.18
7	0.43	0.18	7	0.39	0.17
6	0.43	0.18	6	0.38	0.17

Results show how performance of correlation varies with the number of factors used as well as the number of subjects. Different columns are shown to illustrate the importance of taking into consideration the number of subjects used as this has major impact on the performance seen.

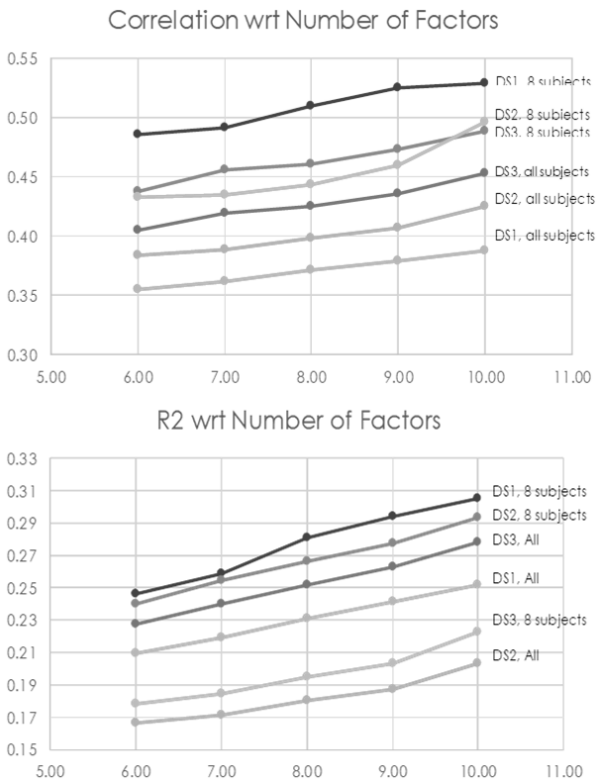

Fig. 3 Matching improves with increase in number of factors

V. Discussions

A. Summary of Findings

The results show here demonstrated that explaining connectivity patterns via significant representatives using a simple linear framework is feasible despite the complexity of the brain network and low signal-to-noise ratio. Not only is the performance comparable to the best in this field but its performance could potentially be further enhanced by exploring the addition of more factors.

B. Applications and Future Work

There are a few future directions that this model can take. Firstly, further efforts could be taken to provide a more holistic approach to optimize the search for hubs with the aim not only limited to enhancing the correlation performance further but also to improve the biophysical interpretation underneath the choices.

Secondly and not entirely mutually exclusive from the first is that multiple connectivity linkages provide an ecosystem which can be monitored and any deviation from a "healthy" ecosystem may signal a display of anomalous characteristic. This makes it a potential useful method for discovery of biomarkers.

Finally, it is easy to try to blend this model with other models. For example, different ROIs can be simulated coherently via this framework and be placed as inputs into more complex diffusion frameworks and processes. The list is far from exhaustive since the model is so generic and simple and can be morphed easily for different purposes.

C. Limitations and Shortfalls

At its present form, the model is not without its various limitations.

Large variance in performance. On average, the correlation is around 0.38~0.45 for the different datasets but within each dataset, this can range from 0.2 to 0.6 for different individuals. This large variance is not desirable as it means some subjects might have low matches (M1<0.3). There are two ways to improve the situation – one is to try to reduce the variance due to subject variability or the other way is to accept the large variance and try to raise the mean level further. Raising the mean level can be easily achieved by improving the search for factors or a combination of improving the search and increasing the number of factors. Based on experience from trial and error, increasing factors is likely to provide quick and short-term benefits while improving global search strategy is likely to yield more lasting long-term benefits.

Out of sample performance. Currently, the model still needs to improve its out of sample performance. The main determinant of out-of-sample performance is how well one set of parameters from training set works on a non-trained set and this is affected by how different the two sets are. There are two kinds of differences. One kind arises from the natural variance in brain functional connectivity; the other is due to man-made nuisance effects that have crept into the dataset because of the way the experiments are set up. The lesser the model is susceptible to the second kind of difference through a more robust process pipeline, the better will be its potential for practical day to day usage.

Resolution. The resolution that is being used currently is [10mm x 10mm x 10mm]. Increasing this resolution increases computation burden without necessarily providing practical improvement in insights. Theoretically, the accuracy of the current search is affected because of scanning at a rougher scale. However, as Fig. 4 shows, the general connectivity patterns are not really affected much even after reducing the resolution.

Model consistency. The model also needs more fine tuning in terms of consistency as showed in Table II. The table basically illustrates the different levels of consistency in factor choice when different datasets are used. Consistency in factor choice can be as high as 70% but once weights or coefficients are considered, consistency drops below 50%. This is expected as consistency in factor choices is normally easier to achieve than consistency in weights.

Inter-subject variability. Perhaps, the most visible shortfall is the decrease in performance when increasing in the number of subjects as seen in Fig. 5. This drop can be made up for to some extent by increasing in factors as well as improving factor search strategy. However, more comprehensive and careful exploration is required to test how much can be improved.

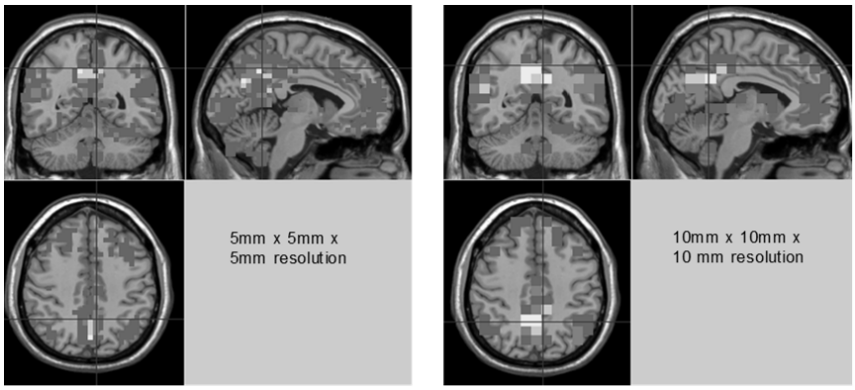

Fig. 4 Functional connectivity with Posterior Cingulate Cortex as seed voxel. One can see the strong resemblances between in connectivity patterns even though the resolutions are different. This provides justification for performing analysis first at a lower resolution and then making suitable refinements and adjustments for high resolution when needed

TABLE II.A
ALIGNMENT BETWEEN ON MODELS BASED ON DS1 AND DS2

#Hubs	Factor choice	Coefficient alignment
10	71.6	41.4
9	73.7	40.0
8	74.6	38.5
7	76.2	37.8
6	78.8	37.2

TABLE II.B
ALIGNMENT BETWEEN ON MODELS BASED ON DS3 AND DS1

#Hubs	Factor choice	Coefficient alignment
10	67.6	61.9
9	69.6	60.9
8	71.3	60.9
7	72.9	58.5
6	75.1	59.6

TABLE II.C
ALIGNMENT BETWEEN ON MODELS BASED ON DS2 AND DS3

#Hubs	Factor choice	Coefficient alignment
10	65.2	50.2
9	67.4	49.5
8	68.9	47.7
7	69.9	44.1
6	72.1	42.8

Model stability (%). This table illustrates the degree of alignment when the same set of factors are calibrated with different datasets. There are 2 types of alignment measured here, namely, factor alignment and coefficient alignment. Factor alignment measures the chance where two datasets choose the same set of factors. Coefficient alignment measures the chance where coefficients cannot be proven to be statistically different from each other for the same factor. One can see that the factor alignment rate is in the range of 65%~75% and expectedly, the smaller number of factors, the higher the alignment rate. Coefficient alignment is harder to achieve compared to factor alignment as weights might vary even for the same set of factors for different subjects. As expected, coefficient alignment is highest between DS1 and DS3 as they came from the same primary data sets.

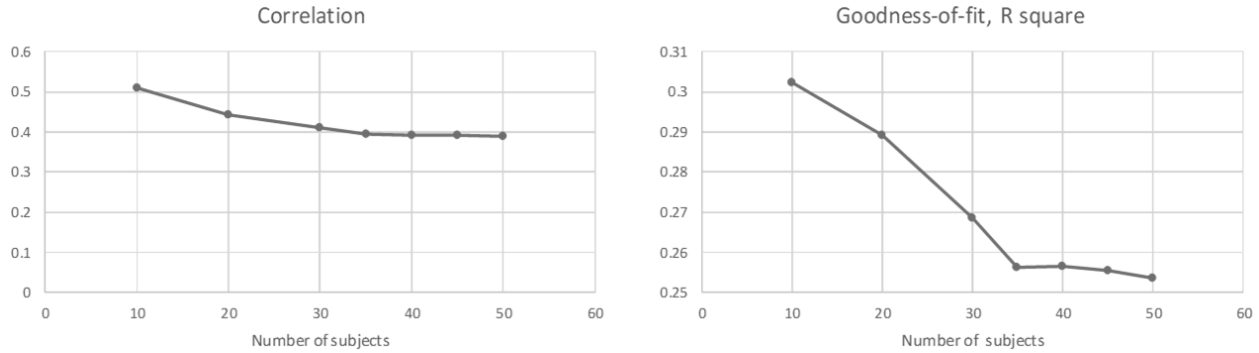

Fig. 5 Variation of performance and fit with number of subjects. The figures above show that the correlation performance is relatively stable given the size of subjects used (>35). Some of the figures noted in previous research in this field must be carefully considered as they still lack the necessary sample size for stability

D. Conclusions

The multivariate linear regression model proposed here shows that it is both possible to be simple and effective when it comes to modeling functional connectivity. The proposed model achieves a performance which is superior to current batch of models in this area.

Two key weaknesses of the model are its weaker out-of-sample performance when compared to in-sample performance as well as the visible decrease in performance when large sample size is used. However, raising the correlation performance of in sample testing tends to improve the performance of out-of-sample testing and make this less conspicuous. For example, if in-sample correlation rising to

0.6 results in out-of-sample correlation rising to 0.5, then, one may be readier to overlook such a weakness. Increasing number of factors as well as improving global search method for hubs are likely strategies that will yield results.

Despite of its limitations, the current model is still very useful if its usage is restricted to only in-sample calibration and by planning the process pipeline carefully to avoid the introduction of nuisance factors as much as possible.

REFERENCES

[1] M. D. Fox, & M. E. Raichle, "Spontaneous fluctuations in brain activity observed with functional magnetic resonance imaging," *Nature Reviews Neuroscience*, 8(9), 2007a.

[2] C. Chang, & G. H. Glover, "Time-frequency dynamics of resting-state brain connectivity measured with fMRI," *NeuroImage*, 2009.

[3] F. Abdelnour, H. U. Voss, & A. Raj, "Network diffusion accurately models the relationship between structural and functional brain connectivity networks," NeuroImage, 90, 2014, pp. 335-347.

[4] R. F. Galán, "On how network architecture determines the dominant patterns of spontaneous neural activity (spontaneous activity patterns)," *PLoS ONE*, 3(5), 2008.

[5] C. J. Honey, O. Sporns, L. Cammoun, X. Gigandet, J. P. Thiran, R. Meuli, & P. Hagmann, "Predicting human resting-state functional connectivity from structural connectivity," *Proceedings of the National Academy of Sciences of the United States of America*, 106(6), 2009.

[6] S. A. Ross "The arbitrage theory of capital asset pricing," *Journal of Economic Theory*, 1976.

[7] R. M. Bilder, F. W. Sabb, T. D. Cannon, E. D. London, J. D. Jentsch, D. S. Parker, N. B. Freimer, "Phenomics: The systematic study of phenotypes on a genome-wide scale," Neuroscience, 164(1), 2009.

[8] D. Wang, D. Liu, S. Li, & Y. Zang, "Increased local synchronization of resting-state fMRI signal after episodic memory encoding reflects off-line memory consolidation," Neuroreport, 23(15), 2012.

[9] C. Yan, & Y. Zang, "DPARSF: A MATLAB toolbox for pipeline data analysis of resting-state fMRI," Frontiers in Systems Neuroscience, 2010.

[10] K. J. Friston, A. P. Holmes, K. J. Worsley, J. - Poline, C. D. Frith, & R. S. J. Frackowiak, "Statistical parametric maps in functional imaging: A general linear approach," *Human Brain Mapping*, 2(4), 1994.

[11] X. Song, Z. Dong, X. Long, S. Li, X. Zuo, C. Zhu, Y. Zang, "REST: A toolkit for resting-state functional magnetic resonance imaging data processing (resting-state fMRI toolkit)," *PLoS ONE*, 6(9), 2011b.